INVESTIGATION OF EFFECT OF SILVER COATING ON MICROSTRIP ANTENNA ARRAYS

K. Prahlada Rao[*], R.M. Vani[**], P. V. Hunagund[*]

[*]Department of PG Studies and Research in Applied Electronics, Gulbarga University
Gulbarga, India 585106
pra_kaluri@rediffmail.com

[**]University Science Instrumentation Centre, Gulbarga University
Gulbarga, India 585106

Abstract

In this paper the effect of silver coating on the performance of microstrip antenna array is examined. The conventional four element microstrip antenna array is producing narrow bandwidth of 4.89 % and high values of mutual coupling of -16.95, -14.22 and -17.30 dB respectively. The modified microstrip antenna array is producing enhanced bandwidth of 31.43 % and reduced mutual coupling of -29.45, -32.71 and -29.94 dB respectively. In addition, good amount of reduction in backward power and increase of forward power indicate improved performance of modified microstrip antenna array. The microstrip antenna arrays are designed using Mentor Graphics IE3D software. The thickness of silver deposition is equal to 30 nm. The conventional microstrip antenna array designed at 6 GHz is resonating at 5.53 GHz with a return loss of -21.12 dB. The dielectric substrate used to design and fabricate microstrip antenna arrays is FR-4 glass epoxy. The measured results of the fabricated antenna arrays are obtained using vector network analyzer.

1. INTRODUCTION

Microstrip antennas and arrays have created a new dimension in the field of antennas. These antennas are suitable for applications in wireless communications, radar technology, satellite communications etc. These antennas have dielectric substrate placed in between the radiating patch and ground plane. Microstrip antennas are characterized by ease of compatibility with other circuits and devices, ease of fabrication, low cost etc. On the other hand, they possess narrow bandwidth and surface wave excitation in the dielectric substrate. Narrow bandwidth implies less amount of information can be

transmitted. Surface wave excitation leads to high values of interference levels between the antenna elements. [1-7].

In [8], D. N. Elsheak *et al* have discussed the study of EBG structures loaded in the ground plane, their types, and their behavior in enhancing the performance of two element microstrip patch antenna arrays. The EBG structures employed are of two dimensional in nature and corporate feeding technique is used to feed the antenna array. The performance of Square, Circular, Star, H and I shape EBG structures are compared. Highest bandwidth of 5.1 % has been achieved using H shape EBG structure. Least amount of mutual coupling (S21) of -30 dB and highest gain of 13.75 dB have been obtained in the case of Star EBG structure. In [9], Fabio Urbani *et al* have reported the performance of microstrip antenna with an iron film patch of ultra-thickness 10 nm. The antenna is fabricated on a double side polished silicon substrate. The antenna is seen to show a response peak greater than 10 dB at 14.5 GHz. The ultra-wide bandwidth produced is equal to 1 GHz. Iron wire with 127 μm diameter and 99.999 % purity is used as the catalyst source. In [10], Maria Roo Ons *et al* have designed a transparent microstrip patch mounted on the surface of a solar module in the 3.5 GHz band. The patch has a thin sheet of clear polyester with an amorphous silicon coating. The measured bandwidth is found to be 154 MHz for the transparent patch and 302 MHz for the copper patch. The corresponding 10 dB bandwidths are equal to 4.3 and 8.3 % respectively. The gain values for the transparent and copper patches are equal to 3.96 and 5.8 dB respectively. The corresponding radiation efficiencies are 50 and 76 % respectively. In [11], Fabio Urbani *et al* have reported on experimental characterization of microstrip antennas with the radiating patch composed entirely of nano films. The four radiating patches are chromium and aluminum each of 15 nm thick, nickel and titanium each of 20 nm thick. The nano films are excited through aperture coupled feeding method. As per the return loss plot, only aluminum thin film patch structure can be classified as antenna. The other structures are classified as resonators. The aluminum thin film structure is producing bandwidth of 660 MHz. The performance of aluminum thin film structure is further investigated using over the air performance to measure the magnitude and direction of radiated energy. The antenna showed a gain of 5 dBi and good radiation properties. In [12], Jai Verdhan Chauhan *et al* have proposed a nano dot antenna array

operating in the frequency range 30 – 70 GHz. Epoxy resin is used as substrate. Two microstrips are present in the centre of the substrate, one lengthwise and the other width wise. The other epoxy substrate is used to make the sandwich. An array of nine nanodots of gold material of radius 100 nm is deposited on the surface of second substrate. The antenna is found to resonate at three frequencies – 38, 48 and 67 GHz respectively. An impedance bandwidth of 2 – 3 GHz is produced. The proposed antenna can be used for wide band applications. In [13], Rajendra Patil *et al* have reported experimental characterization of microstrip patch antenna with silver nanofilm of thickness 30 nm. The silver radiating nano film is fed by proximity coupled feeding technique. The silver nano film is deposited on top of circular radiating patch. An enhanced bandwidth of 2.71 GHz (22.39 %) with return loss of -20.41 dB is obtained at the resonant frequency of 12.1 GHz. The factors contributing to the increase in bandwidth are increase in surface resistance and skin depth. In [14], Arshad Hassan *et al* have reported the design of of a high gain antenna operating over dual band of 900 MHz and 2.4 GHz using conductive ink of silver nanoparticles to print the proposed antenna on 50 microns thick, transparent and flexible polyethyleneterephthalate (PET) substrate. The antenna structure comprises of Z-shaped radiating monopole antenna fed by co-planar waveguide feeding technique. The PET substrate has dielectric constant of 2.8 and loss tangent of 0.003. High gains of 16.74 and 16.24 dBi are obtained at 900 MHz and 2.4 GHz respectively. The fractional bandwidths obtained at the corresponding frequencies are 23.33 and 11.66 % respectively. The proposed antenna is well suited for wearable devices requiring dual Wi-Fi band. In [15], S. A. Mohasseib *et al* have studied the performance of a low-profile wide band waveguide fed monopole antenna at 20 GHz and printed using silver nanoparticle ink on polyethyleneterephthalate and Epson paper substrates. A conductivity of 1.8 × 107 S/m is obtained leading to superior antenna performance with gain and antenna radiation efficiency of 1.67 dB and 96 %. Using antenna on Epson paper substrate is showing bandwidth extending from 17.18 – 24.3 GHz leading to a fractional bandwidth of 34.34 %. In [16], Mahesh C. P *et al* have designed microstrip antenna for wireless applications by loading zinc nanoparticles on rectangular patch of proposed antenna. The nano antenna is resonating at five frequencies and their corresponding bandwidths are 3.4 – 3.9 GHz (13.88 %), 4.2 – 5.2 GHz (22.22 %), 5.5 – 7.1 GHz (26.44 %), 7.6 – 8.8 GHz

(16 %) and 8.95 – 9.4 GHz (4.97 %) respectively. Gain of the antenna is enhanced to 5 dB. In [17], Mahesh C. P *et al* have designed microstrip antenna of equilateral triangular radiating patch with iron nanoparticles loaded on the patch. The nano antenna is resonating at four frequencies and their corresponding bandwidths are 3.9 – 4.05 GHz (3.65 %), 5.9 – 6.3 GHz (6.55 %), 6.9 – 8.8 GHz (26.02 %) and 9.5 – 12 GHz (22.12 %) respectively. Gain of the antenna is enhanced to 5.12 dB. In [18], Seung Yoon Lee *et al* have performed a review on transparent nano patterned antennas classified by various materials in terms of optical transmittance and sheet resistance. Graphene nano carbon-based patch antennas designed in microwave frequency are producing radiation efficiency of 8 %. On the other hand, using plasmonic propagation in the THz frequency are yielding antenna efficiency of 60 %. Onion like carbon and multi wall carbon nano tube film-based dipole antennas are exhibiting peak gains of -1.48 and -2.76 dBi. The copper film-based antenna is featuring a peak gain of 3.5 dBi at 2.4 GHz. Transparent conductive oxides (TCO) based antennas with four films (ITO, FTO, AgHT-4, AgHT-8) with sheet resistances of 10, 24, 4.5 and 8 Ω/sq are showing wide bandwidth property. FTO is providing the highest bandwidth while ITO is giving the best performance of return loss.

2. MATERIALS AND METHODS

In the first step, conventional microstrip antenna array (CMAA) is designed. The design frequency of CMAA is 6 GHz. FR-4 glass epoxy is employed as dielectric substrate which has dielectric constant of 4.2 and loss tangent of 0.0245. The height of the dielectric substrate is 1.6 mm. CMAA has four identical rectangular radiating patches fed by corporate feeding technique. The adjacent radiating patches of CMAA are separated by quarter wavelength, where the wavelength is calculated at the design frequency of 6 GHz. The dimensions of the patch are 15.73 mm × 11.76 mm. The schematic of CMAA is depicted in Figure 1. The schematic in Figure 1 is used to determine the return loss characteristics of CMAA.

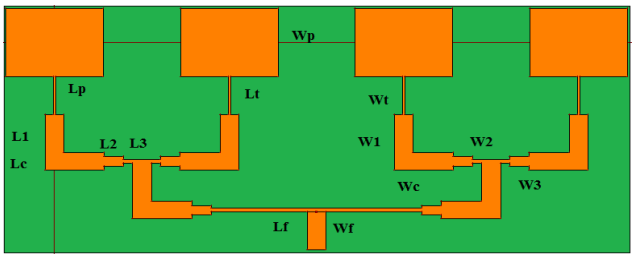

Figure 1. Schematic of CMAA.

All the dimensions of CMAA are depicted in Table 1.

Table 1. Dimensions and values of CMAA.

Dimension	Value (mm)
Length of the patch (Lp)	15.73
Width of the patch (Wp)	11.76
Length of the quarter wave transformer (Lt)	6.47
Width of the quarter wave transformer (Wt)	0.47
Length of the 50Ω line (L1)	6.52
Width of the 50Ω line (W1)	3.05
Length of the coupler	3.05
Width of the coupler	3.05
Length of the 70Ω line (L2)	6.54
Width of the 70Ω line (W2)	1.62
Length of the 100Ω line (L3)	6.56
Width of the 100Ω line (W3)	0.70
Length of the feed line (Lf)	6.52
Width of the feed line (Wf)	3.05

By maintaining the same distance between the two adjacent antenna elements as λ/4, the parameter mutual coupling can be measured by exciting the four antenna elements separately as shown in Figure 2. All the four antenna elements are assumed to be fed with the same amount of power.

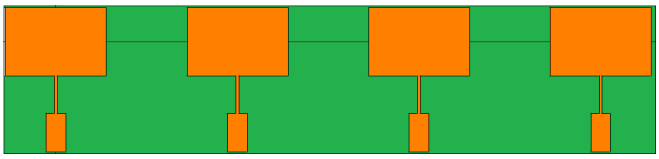

Figure 2. Schematic of setup of CMAA for mutual coupling measurement.

The proposed microstrip antenna array (PMAA) is designed by modifying CMAA in such a way that a thin layer of silver material is placed on top of the entire copper area of CMAA. The schematic of PMAA is depicted in Figure 3. The thickness of silver

deposited is equal to 30 nm. The grey part of the schematic in Figure 3 indicates the silver coating on top of entire copper area. The schematic in Figure 3 is used to evaluate the return loss characteristics of PMAA.

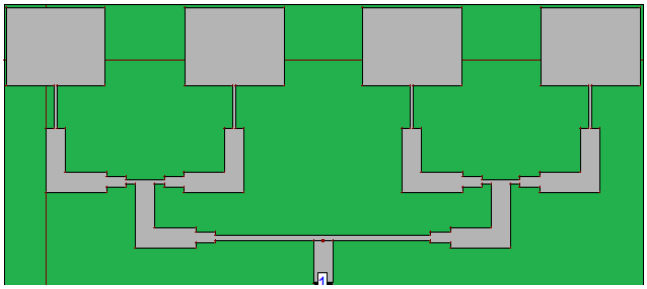

Figure 3. Schematic of PMAA.

To measure the mutual coupling values of PMAA, silver material of thickness 30 nm is deposited on the entire copper area of schematic of Figure 2. Figure 4 shows the schematic employed to determine the variation in mutual coupling values after the deposition of silver coating. In Figure 4 the grey part shows the silver placed on top of entire copper area.

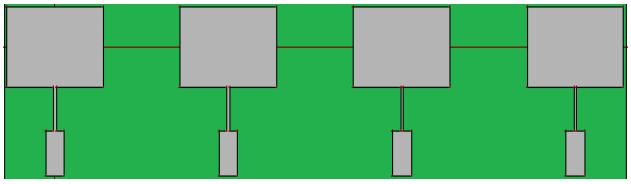

Figure 4. Schematic of setup of PMAA for mutual coupling measurement.

Figures 5, 6, 7 and 8 depict the photographs of the fabricated microstrip antenna arrays.

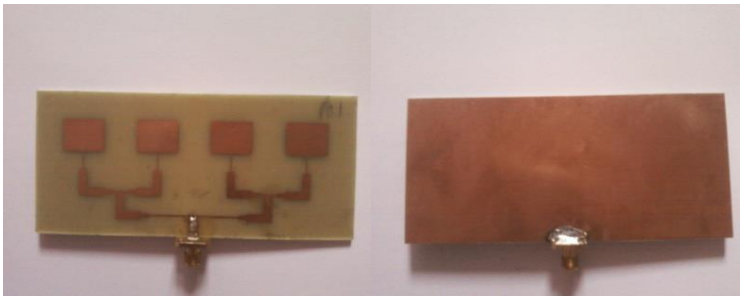

Figure 5. Photograph of fabricated CMAA.
(a) Front view (b) Back view.

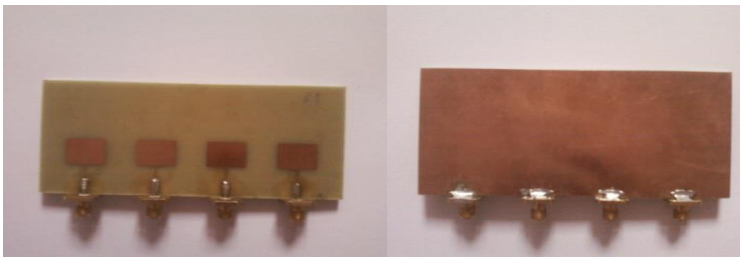

Figure 6. Photograph of fabricated setup of CMAA for mutual coupling measurement.
(a) Front view (b) Back view.

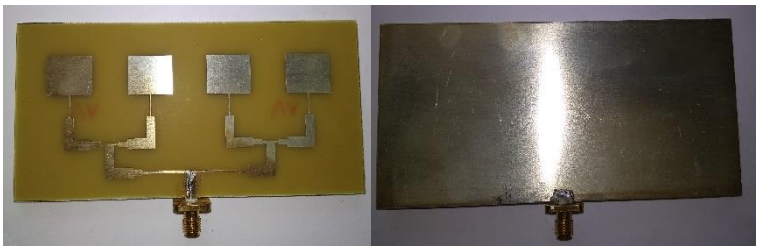

Figure 7. Photograph of fabricated PMAA.
(a) Front view (b) Back view.

Figure 8. Photograph of fabricated setup of PMAA for mutual coupling measurement.
(a) Front view (b) Back view.

3. RESULTS AND DISCUSSIONS

The performances of CMAA and PMAA are differentiated in terms of parameters – resonant frequency, return loss, mutual coupling, forward and backward powers. The measured results are obtained using vector network analyzer. Figures 9, 10 and 11 depict the graphs of measured return loss and mutual coupling characteristics versus frequency of CMAA. The return loss is designated by the S-parameter S11.

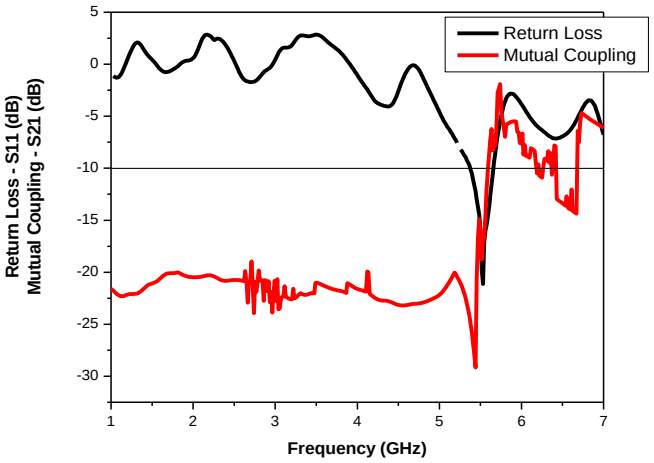

Figure 9. Plot of return loss and mutual coupling – S21 versus frequency

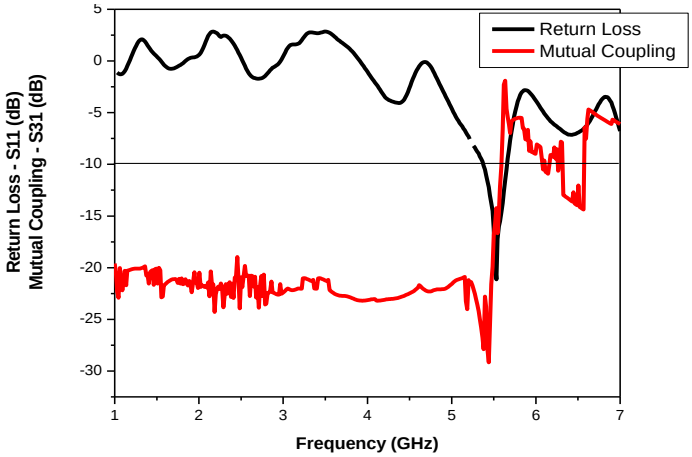

Figure 10. Plot of return loss and mutual coupling – S31 versus frequency of CMAA.

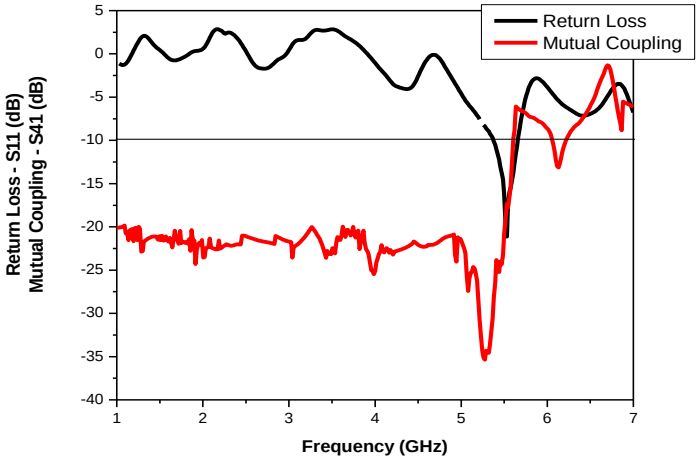

Figure 11. Plot of return loss and mutual coupling – S41 versus frequency of CMAA.

Figures 9, 10 and 11 show that CMAA is resonating at the fundamental frequency of 5.53 GHz. The return loss produced at the resonant frequency of 5.53 GHz is equal to -21.12 dB. From the return loss graph the parameter bandwidth is calculated. The lower frequency is subtracted from upper frequency where the return loss is equal to – 10 dB to calculate the bandwidth. The lower and upper frequencies are located on either side of the resonant frequency. Therefore the bandwidth of conventional microstrip antenna array is equal to 273 MHz. The bandwidth (%) is determined by using equation (1)

$$\frac{Bandwidth}{Resonant\ frequency} \times 100\% \tag{1}$$

Hence, CMAA is producing bandwidth of 4.89 %. As the bandwidth of CMAA is very narrow it is very much required to enhance it.

From Figures 9, 10 and 11 we see that the measured values of mutual coupling (S21, S31 and S41) of CMAA are -16.95, -14.22 and -17.30 dB respectively. The values of mutual coupling are very high and detrimental and need to be decreased. Additionally, we can see that the graphs of return loss and mutual coupling versus frequency of CMAA are crossing each other at the resonant frequency of 5.53 GHz. This means that there is interference between the transmitting element 1 and the receiving elements 2, 3 and 4 respectively of CMAA. Hence there is no proper transmission and reception of information between the transmitting element 1 and the receiving elements 2, 3 and 4 of CMAA.

Figures 12, 13 and 14 depict the graphs of return loss and mutual coupling versus frequency of PMAA.

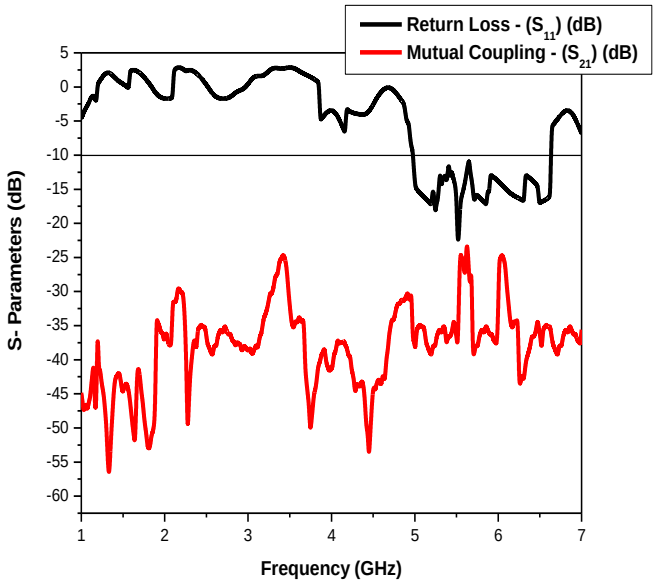

Figure 12. Plot of return loss and mutual coupling – S21 versus frequency of PMAA.

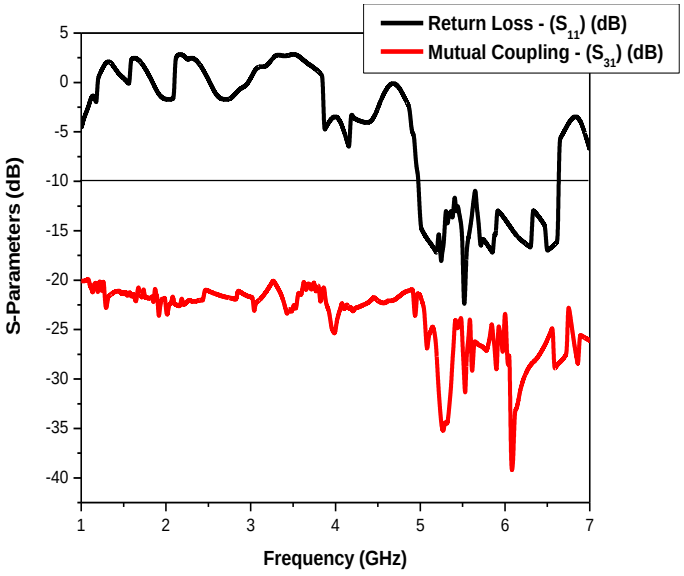

Figure 13. Plot of return loss and mutual coupling – S31 versus frequency of PMAA.

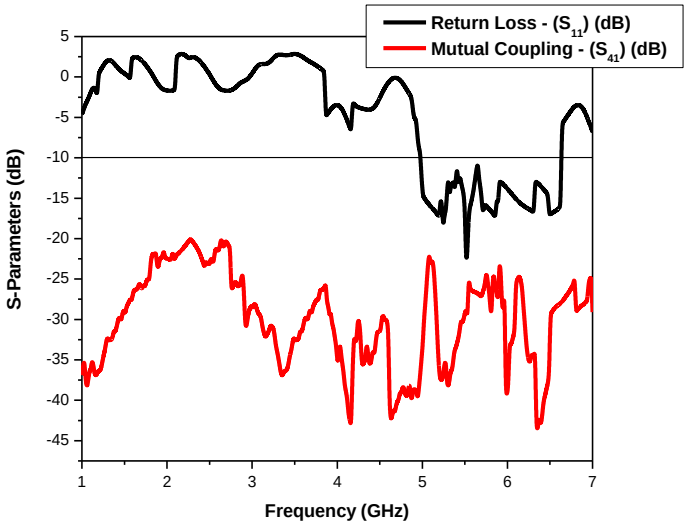

Figure 14. Plot of return loss and mutual coupling – S41 versus frequency of PMAA.

The graphs in Figures 12, 13 and 14 depict that PMAA is resonating at fundamental frequency of 5.53 GHz. The return loss produced at the resonant frequency of 5.53 GHz is equal to -22.45 dB. The bandwidth obtained is equal to 1.73 GHz. Therefore, the bandwidth (%) of PMAA is equal to 31.43 %. Hence the bandwidth (%) of PMAA of 31.43 % is greater than that produced by CMAA equal to 4.89 %. Therefore, PMAA is a better antenna than CMAA in terms of bandwidth.

From Figures 12, 13 and 14 we see that the measured values of mutual coupling (S21, S31 and S41) of PMAA are -29.45, -32.71 and -29.94 dB respectively. The values of mutual coupling are decreased with the introduction of silver coating. Additionally, we can also see that the graphs of return loss and mutual coupling versus frequency are not overlapping each other at the resonant frequency of 5.53 GHz. This means that there is less interference between the transmitting element 1 and the receiving elements 2, 3 and 4 respectively in PMAA compared to that in CMAA. Hence there is better transmission and reception of information between the transmitting element 1 and the receiving elements 2, 3 and 4 in PMAA compared to that in CMAA. Hence PMAA is a better candidate than CMAA in terms of mutual coupling.

The radiation patterns of CMAA and PMAA are shown in Figure 15.

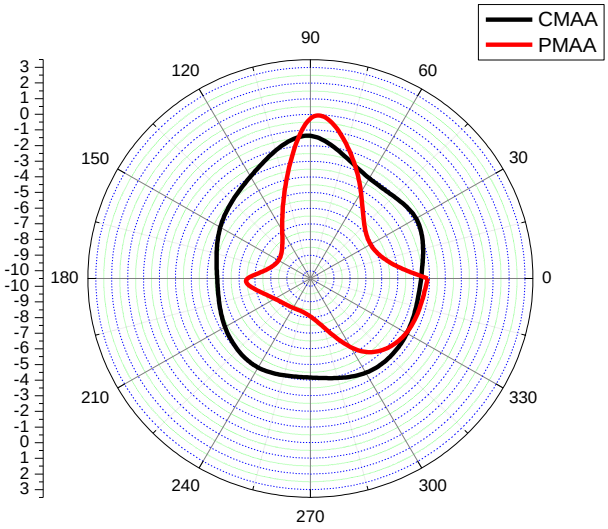

Figure 15. Plot of radiation patterns of CMAA and PMAA.

The forward power radiated is measured at the angle of 90^o and the backward power at the angle of 2700. In the case of CMAA the forward and backward powers measured are equal to -2 and -4.5 dB respectively. The corresponding powers radiated by PMAA -0.5 and -8 dB respectively. We see that PMAA is radiating increased power in the forward direction and lesser power in the backward direction compared to its counterpart i.e. CMAA. Hence PMAA is a better radiator than CMAA in terms of forward and backward powers.

Front to back ratio is calculated by using deducting the power radiated in the backward direction from the power radiated in the forward power.

The calculated values of front to back ratio of CMAA and PMAA are equal to 2.5 and 7.5 dB. As front to back ratio of PMAA is greater than that of CMAA, PMAA is a better antenna in terms of front to back ratio.

As PMAA is performing better than CMAA in terms of bandwidth, mutual coupling, front power, backward radiation and front to back ratio, hence PMAA is considered as a superior candidate compared to CMAA.

Table 2 depicts the summarized measured results of CMAA and PMAA.

Table 2. Summarized measured results of CMAA and PMAA.

Type of Antenna	Resonant Frequency (GHz)	Return Loss (dB)	Band Width (MHz)	Band Width (%)	Mutual Coupling (dB)
CMAA	5.53	-21.12	273	4.89	-16.95 -14.22 -17.30
PMAA	5.53	-22.45	1730	31.43	-29.44 -32.71 -29.94

4. CONCLUSION

In this paper, the study of performance of four element antenna array without and with silver coating is performed in terms of various parameters. The antenna arrays have been successfully designed and tested practically. The simulated and experimental results are in agreement to a good extent. The deposition of silver coating is producing enhanced bandwidth and good reduction in mutual coupling values. With reduction in back lobe power, the introduction of silver coating demonstrates the enhanced performance of proposed microstrip antenna array compared to its counterpart i.e. conventional microstrip antenna array. The proposed microstrip antenna array finds application in the C band of the microwave frequency range.

REFERENCES

[1] Constantine A Balanis; Antenna Theory, Analysis and Design, John Wiley & Sons Inc 2nd edition.1997.

[2] I. J. Bahl and P. Bhartia; Microstrip Antennas, Artech House. 1980.

[3] https://www.nanowerk.com/nanotechnology/introduction/introduction_to_nanotechnology_1.php.

[4] Mentor Graphics IE3D User Manual, 2010.

[5] James Scott; Lecture Notes of EEET 1071/1127 Microwave and Wireless Passive Circuit Design. 2004.

[6] L.I. Maissel, R.G. Glang; Handbook of Thin Film Technology, McGraw-Hill Book Company, New York, USA. 1970.

[7] A. K. Gautam; Antenna and Wave Propagation, 5th edition. 2010.

[8] D. N. Elsheakh, E. A. Abdallah, M. F. Iskander and H. A. Elsadek, "Microstrip Antenna Array with New 2D-Electromagnetic Band Gap Structure Shapes to Reduce Harmonics and Mutual Coupling", Progress in Electromagnetic Research C, Vol.12, pp. 203-213,2010.

[9] Fabio Urbani, David W. Stollberg and Amit Verma, "Outstanding Performance of a Nanofilm Microstrip Antenna", Proc. of 2010 IEEE Nanotechnology Materials and Devices Conference, Monterey, California, USA, Oct 12-15, pp. 160-163, 2011.

[10] Maria Roo Ons, S. V. Shynu, Max Ammann, Sarah McCormak and Brian Norton, "Transparent Patch Antenna on a Si Thin Film Glass Solar Module", Electronic Letters, Vol. 47, Issue. 2, pp. 85-86, 2011.

[11] Fabio Urbani, David W. Stollberg and Amit Verma, "Experimental Characterization of Nanofilm Microstrip Antennas", IEEE Transactions on Nanotechnology, Vol. 11, Issue. 2, pp. 406-411, Mar 2012.

[12] Jai Verdhan Chauhan, Abhishek Khandwal and Sunil Kumar Khah, "High Frequency Multilayer Equally Spaced Nano Dot Antenna Array", International Journal of Emerging Technology and Advanced Engineering, Vol.4, Special Issue 1, pp. 336-338, Feb.2014.

[13] Rajendra R. Patil, Vani R. M and P. V. Hunagund, "Experimental Characterization of Silver Nanofilm Proximity Coupled Microstrip Patch Antenna", International Journal of Engineering Trends and Technology, Vol. 13, Issue. 6, pp. 299-302, Jul.2014.

[14] Arshad Khan, Shawkat Ali, Gul Hassan, Jinho Bae and Chong Hyun Lee, "Ink-Jet Printed Antenna on Thin PET Substrate for Dual Band Wi-Fi Communications", Microsystem Technologies, Aug. 2016.

[15] S. A. Mohasseib, Khaled Kirah, Edgar Dorsam, Ahmed S. G. Khalil and Hadia M. El- Hennawy, "Effect of Silver Nanoparticle Ink Drop Spacing On The Characteristics of Coplanar Waveguide Monopole Antennas Printed on Flexible Substrates", IET Microwaves, Antennas & Propagation, Vol. 11, Issue. 11, pp. 1572-1577, 2017

[16] S Mahesh C. P, Madhuri Chavan, Maheshwar Sharon and Madhuri Sharon, "Design and Fabrication of Rectangular Microstrip Antenna Using Zinc Nanoparticles for

Wireless Applications and Enhancement of Bandwidth", International Journal for Research in Applied Science & Engineering, Vol. 6, Issue. 5, pp. 249-252, May 2018.

[17] Mahesh C. P, Pooja Mali, Maheshwar Sharon and Madhuri Sharon, "Enhancement of Bandwidth of Equilateral Triangular Microstrip Antenna Using Nanoparticles", International Journal for Research in Applied Science & Engineering, Vol. 6, Issue. 5, pp. 257-260, May 2018.

[18] Seung Yoon Lee, Moogoong Choo, Sohyeon Jung and Wonbin Hong, "Optically Transparent Nano-Patterned Antennas: A Review and Future Directions", Applied Sciences, Vol. 8, pp. 1-13, May 2018.